

Models for the Relativistic Electron Population and Nonthermal Emission in Clusters of Galaxies

Craig L. Sarazin

Department of Astronomy, University of Virginia, P. O. Box 3818, Charlottesville, VA 22903-0818, U.S.A.

Abstract. Models for the integrated relativistic electron population in clusters of galaxies are presented. The results depend on the history of electron acceleration in the cluster. If there is no present particle acceleration or other sources, then no high energy electrons ($\gamma \gtrsim 300$, $E \gtrsim 150$ MeV) should be present due to inverse Compton (IC) losses. High energy electrons are present if particle acceleration is occurring at present, perhaps as a result of a cluster merger shock. The resulting IC, synchrotron, and gamma-ray emission from these models has been calculated. In the models, extreme ultraviolet (EUV) and very soft X-ray emission are a nearly ubiquitous feature, because this emission comes from IC by electrons with the longest lifetimes in clusters. Diffuse UV and optical emission is also expected in most clusters, but at levels which will be difficult to observe. Hard X-ray tails and diffuse radio synchrotron emission are only expected in clusters with recent or current particle acceleration; for example, this acceleration might be due to intracluster merger shocks. Gamma-ray observations at energies of around 100 MeV should detect both the dominant population of relativistic electrons and the corresponding ions. The predicted fluxes are easily detectable with GLAST.

1. Introduction

There are a number of reasons to think that cosmic ray particles might be particularly abundant within the intracluster medium. First, clusters of galaxies should be very effective traps for cosmic ray ions and electrons. Under reasonable assumptions for the diffusion coefficient, particles with energies of less than $\lesssim 10^6$ GeV have diffusion times which are longer than the Hubble time (Colafrancesco & Blasi 1999). Second, the lifetimes of cosmic ray particles, even the electrons which are responsible for most of the radiative signatures of relativistic particles, can be quite long. The radiation fields (optical/IR and X-ray) and magnetic fields ($B \lesssim 1 \mu\text{G}$) in the ICM are low enough that high energy electrons mainly lose energy by inverse Compton (IC) scattering of Cosmic Microwave Background (CMB) photons (Sarazin & Lieu

1998). Lower energy electrons can lose energy by Coulomb interactions with the plasma; however, at the very low densities ($n_e \lesssim 10^{-3} \text{ cm}^{-3}$) in the bulk of the ICM, this is only important for electrons with $\gamma \lesssim 200$. (Here, γ is the Lorentz factor for the electrons, so that their total energy is $\gamma m_e c^2$.) For electrons with $\gamma \gtrsim 200$, the lifetime is set by IC losses and is

$$t_{IC} = \frac{(\gamma - 1)m_e c^2}{\frac{4}{3}\sigma_T c \gamma^2 U_{CMB}} \approx 7.7 \times 10^9 \left(\frac{\gamma}{300}\right)^{-1} \text{ yr.} \quad (1)$$

The lifetimes of ions are set by interactions; for protons, this gives $t_{ion} \gtrsim 10^{11} (n_e / 10^{-3} \text{ cm}^{-3})^{-1}$ yr. Thus, clusters of galaxies can retain low energy electrons ($\gamma \sim 300$) and nearly all cosmic ray ions for a significant fraction of a Hubble time.

Clusters of galaxies are likely to have substantial sources of cosmic rays. Clusters often contain powerful radio galaxies, which may produce and distribute cosmic rays throughout the cluster, in addition to possible contributions from the cluster galaxies. However, the primary reason why the cosmic ray populations in clusters might be large is connected with the high temperature of the intracluster gas. This indicates that all of the intracluster medium (typically, $10^{14} M_\odot$ of gas) has passed through strong shocks with shock velocities of ~ 1000 km/s during its history. In our own Galaxy, whenever diffuse gas undergoes a strong shock at velocities of this order, a portion of the shock energy goes into the acceleration of relativistic particles (e.g., Blandford & Eichler 1987). Thus, it seems likely that relatively efficient particle acceleration also occurs in clusters of galaxies.

Direct evidence for the presence of an extensive population of relativistic particles and magnetic fields in the ICM comes from the observation of diffuse synchrotron radio halos in clusters (e.g., Giovannini et al. 1993). More recently, extreme ultraviolet (EUV) and very soft X-ray emission has been detected from a number of clusters (Lieu et al. 1996a,b; Mittaz, Lieu, & Lockman 1998). One hypothesis is that this radiation is inverse Compton (IC) emission by relativistic electrons (Hwang 1997; Enßlin & Biermann 1998; Sarazin & Lieu 1998). Finally, hard X-ray emission has recently been detected in clus-

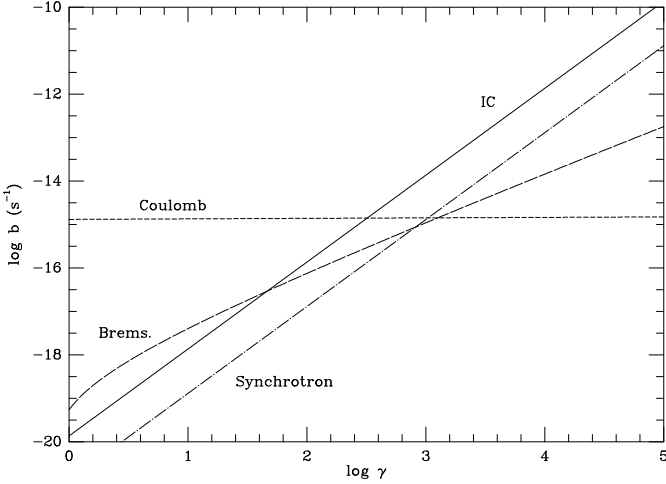


Fig. 1. The values of the losses function $b(\gamma)$ for inverse Compton (IC) emission, Coulomb losses, synchrotron losses, and bremsstrahlung losses as a function of γ . The values assume $n_e = 10^{-3} \text{ cm}^{-3}$, $B = 1 \mu\text{G}$, and $z = 0$.

ters with *BeppoSAX*, which might be due to IC emission from higher energy electrons (Fusco-Femiano et al. 1999; Kaastra, Bleeker, & Mewe 1998). The EUV emission would require electrons with $\gamma \sim 300$, while the hard X-ray emission would require $\gamma \sim 10^4$.

In this paper, illustrative models will be presented for the integrated energy spectrum of primary, relativistic electrons, under the assumption that they remain trapped in the cluster (Colafrancesco & Blasi 1999). More details on these models are given in Sarazin (1999). Radio synchrotron and inverse Compton emission spectra will be determined up to the hard X-ray spectral band. Gamma-ray emission by the same electrons (as well as emission by ions through π^0 decay) will also be discussed briefly.

2. The Electron Spectrum in Clusters

I will use the Lorentz factor γ of the electrons as the independent variable rather than the kinetic energy $E = (\gamma - 1)m_e c^2$, where m_e is the electron mass. Let $N(\gamma)d\gamma$ be the total number of electrons in the cluster with energies in the range γ to $\gamma + d\gamma$, and let $Q(\gamma)d\gamma$ be the total rate of production of new cosmic ray this energy range. The equation for the electron spectrum is then

$$\frac{\partial N(\gamma)}{\partial t} = \frac{\partial}{\partial \gamma} [b(\gamma)N(\gamma)] + Q(\gamma), \quad (2)$$

where $b(\gamma) = -d\gamma/dt$ gives the energy loss by an individual electron.

The loss function includes IC emission, Coulomb losses, synchrotron losses, and bremsstrahlung losses. In Fig. 1, these loss rates are shown as a function of γ for typical cluster conditions. IC losses dominate at high energies $\gamma \gtrsim 200$, while Coulomb losses dominate at low energies. Values for the loss time scale, defined as $t_{loss} \equiv \gamma/b(\gamma)$,

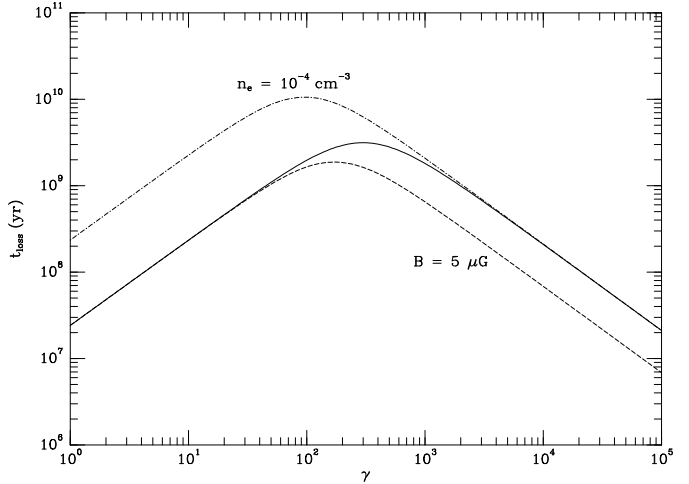


Fig. 2. The solid curve gives the loss time scale t_{loss} as a function of γ for electrons in a cluster with an electron density of $n_e = 10^{-3} \text{ cm}^{-3}$ and a magnetic field of $B = 1 \mu\text{G}$. The short-dash curve is for $B = 5 \mu\text{G}$, while the dash-dot curve is for $n_e = 10^{-4} \text{ cm}^{-3}$.

are shown in Fig. 2. The lifetime are maximum at $\gamma \approx 300$, where they are $\sim 3 - 10$ Gyr, which is comparable to the likely ages of clusters.

The nature of the resulting electron populations depends on whether there is a current or very recent ($z \lesssim 0.03$) source of particles in the clusters, such as an ongoing merger shock, or the electrons were all accelerated in the past ($0.03 \lesssim z \lesssim 1$). In all of the models shown here, the accelerated electrons have a power-law spectrum, $Q(\gamma) = Q_1 \gamma^{-p}$ with $p = 2.3$, and the electron spectra are normalized such that the total kinetic energy injected in electrons with $\gamma \geq 300$ is $E_{CR,e}^{tot} = 10^{63} \text{ ergs}$. Fig. 3 shows the present-day electron spectra in a series of models without any current source of newly accelerated particles. Thus, these models might apply to a cluster which is not currently undergoing a subcluster merger. At low energies, the electron population is reduced and the shape flattened by Coulomb losses. At high energies, the electron population is reduced and the shape of the spectrum steepened by IC and synchrotron losses. Because the IC and synchrotron losses increase with the square of the electron energy, there is an upper cut-off to the electron distribution; no electrons are found at energies higher than γ_{max} . Because the energy density in the CMB increases as $(1+z)^4$, the IC losses increase rapidly at high redshift. If there is no electron acceleration since $z \gtrsim 1$, the value of $\gamma_{max} \lesssim 100$, and Coulomb losses remove all of the lower energy electrons. In order to have any significant population of primary electrons with $\gamma \gtrsim 10^2$ at the present time, there must have been a substantial injection of particles into clusters at moderately low redshifts, $z \lesssim 1$.

Fig. 4 shows the resulting present-day electron spectra in models in which there is a current source of accelerated electrons, such as a cluster merger shock. Again, Coulomb

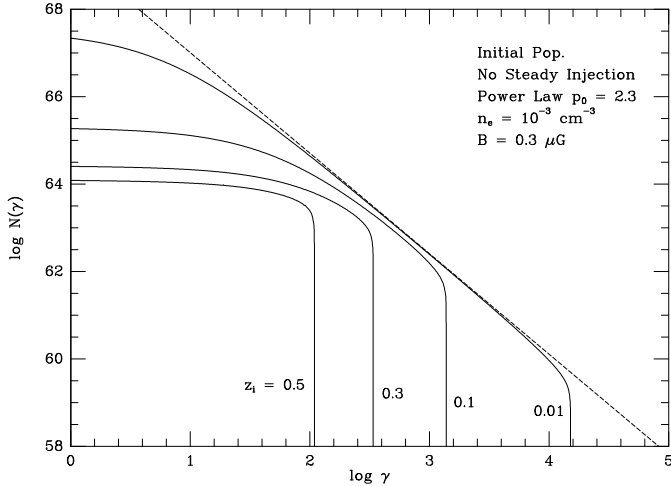


Fig. 3. The present day relativistic electron populations in models with no current particle acceleration (e.g., no subcluster merger at present). An initial population of electrons, which is shown as a dashed line, was introduced into the cluster at a redshift of $z_i = 0.01, 0.1, 0.3$, and 0.5 .

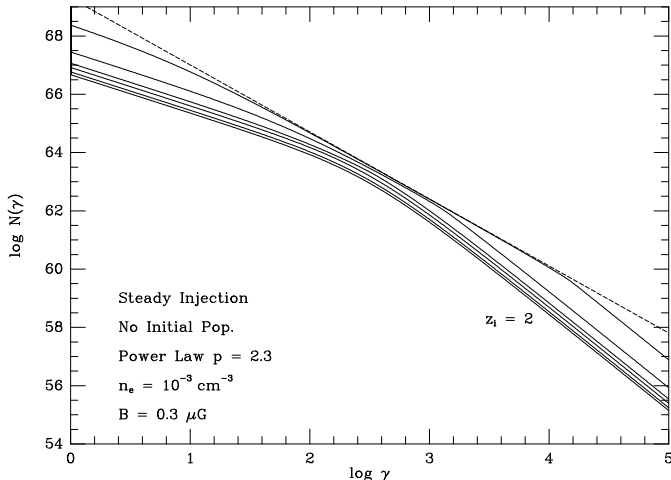


Fig. 4. The present day relativistic electron populations in a series of models with ongoing particle acceleration, perhaps due to a cluster merger shock. The solid curves show models for clusters which started at redshifts of $z_i = 2, 1, 0.5, 0.3, 0.1$, and 0.01 (bottom to top). The short-dashed curve gives the total power-law spectrum of all of the injected particle over the cluster lifetime.

losses reduce and flatten the electron population at low energies, and IC and synchrotron losses reduce and steepen the electron population at high energies. However, these losses don't remove the high energy particles completely, as new particles are always being accelerated. Instead, the population quickly relaxes into steady-state, where the low (high) energy population is one power flatter (steeper) than the injected electrons (Ginzburg & Syrovatskii 1964).

Finally, we consider models in which there is an initial population in the cluster, and in which there also is current injection of new particles. These might apply to the more realistic cases where the cluster had particle acceleration associated with the formation of the cluster and mergers in the past, but also has a subcluster merger occurring at present. An illustrative set of such models are shown in Fig. 5. The different models are characterized by differing values of F_{inj} , which is the fraction of the particle energy which has been injected by the current steady injection process, as opposed to the earlier population. If the electrons were injected in cluster shocks, then F_{inj} might be roughly proportional to the fraction of the thermal energy content of the ICM which is being generated in the current shock. The general features of these models are that the electron spectrum is moderately flat below $\gamma \approx 300$. Unless there is a very strong present merger or other current particle source, the electron population drops off rapidly above $\gamma \approx 300$. In most models for clusters, most of the relativistic electron energy should be in particles with $\gamma \approx 300$; these are the particles with the longest lifetimes (Fig. 2). If a cluster has a ongoing merger or other particle source, then there will also be a high energy tail to the particle distribution. Because this tail is likely to be in steady-state, the electron distribution is likely to be one power steeper than the source, perhaps $N(\gamma) \propto \gamma^{-3.3}$.

3. Inverse Compton Emission

The emission produced by the relativistic electron populations through the inverse Compton scattering of CMB photons was also calculated. Let $L_\nu d\nu$ be the luminosity of IC emission at frequencies from ν to $\nu + d\nu$. Then, the spectrum of IC emission is related to the electron spectrum $N(\gamma)$ by

$$L_\nu = 12\pi\sigma_T \int_1^\infty N(\gamma) d\gamma \int_0^1 J\left(\frac{\nu}{4\gamma^2 x}\right) \mathcal{F}(x) dx, \quad (3)$$

where $\mathcal{F}(x) \equiv 1 + x + 2x \ln x - 2x^2$. Here, $J(\nu)$ is the mean intensity at a frequency ν of the radiation field being scattered. For the CMB, this is just the black body function $J(\nu) = B_\nu(T_{CMB})$. For a power-law electron spectrum $N(\gamma) \propto \gamma^{-p}$, the IC spectrum is a power-law $L_\nu \propto \nu^\alpha$, where $\alpha = -(p-1)/2$. This gives $\alpha = -0.65$ for the injection spectrum $p = 2.3$.

Fig. 6 shows the resulting IC spectra for a variety of different models; for details of the specific models, see Sarazin (1999). Model 1 has a current source of electrons; for example, this might be due to a subcluster merger. At frequencies above 10^{17} Hz, the spectrum quickly steepens with time due to IC losses, and becomes a half power steeper than that given by the injected electron spectrum, $\alpha \approx -(p/2) \approx -1.15$. At low frequencies, the spectrum flattens more gradually due to Coulomb losses, approaching a spectrum which is a half power flatter than that due

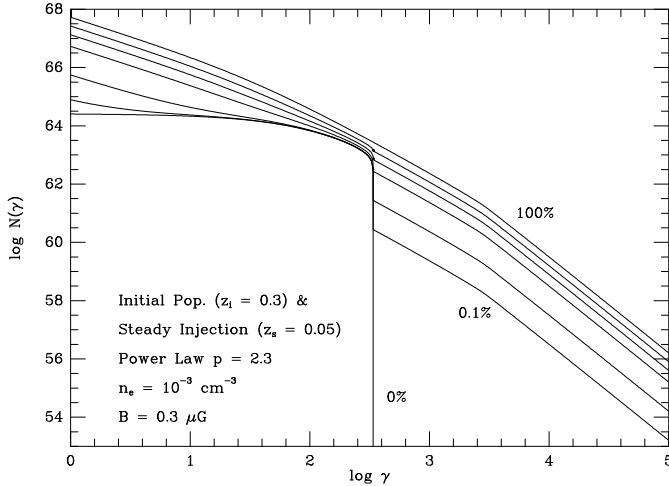


Fig. 5. The electron energy spectra in models with both an initial electron population and current injection of new particles, perhaps due to an ongoing cluster merger. The values of the fraction of particle energy due to current injection are (top to bottom) $F_{inj} = 100\%, 50\%, 25\%, 10\%, 1\%, 0.1\%$, and 0% .

to the injected spectrum, $\alpha \approx -(p-2)/2 \approx -0.15$. If the current acceleration process has occurred since a redshift of $z \gtrsim 0.2$, the spectrum is near that of a steady-state electron population, with these two power-laws meeting at a knee at $\nu \sim 3 \times 10^{16}$ Hz. If the current acceleration process is more recent, there is a central region of the IC spectrum where the electrons are not yet in steady-state. Here, the spectral index is $\alpha \approx -0.65$.

Models 11 and 22 have no current source of electrons (e.g., no ongoing cluster merger). The electron energy distributions of these models have a cut off at high energies, γ_{max} , which results from rapid IC and synchrotron losses by high energy electrons (see Fig. 3). As a result, the IC spectra have a very rapid fall off at high energies (exponentially or slightly faster; see eq. [54] in Sarazin [1999]).

At low frequencies, the IC spectra of models without current acceleration flatten and become slowly increasing with frequency as the models age. We expect that the low energy electron spectrum in an older model without current acceleration will become nearly independent of γ except for a slowly varying logarithmic factor (see eq. 36 in Sarazin [1999]). If $N(\gamma) \approx N_{low} = \text{constant}$ at low energies, then the low frequency IC spectrum varies as $L_\nu \propto \nu^{1/2}$.

Model 27 in Fig. 6 shows the spectrum of a model with both an initial population of particles and electron acceleration at the present time. In this model, the fraction of electron being contributed by the current acceleration (e.g., current merger shock) is $F_{inj} = 1\%$. Models in which the current rate of particle injection provides a small but significant fraction of the total electron energy have hybrid spectra. At low frequencies ($\nu \lesssim 10^{17}$ Hz), they have an extended hump of emission, with a rapid fall off above

$\nu \sim 10^{16}$ Hz. However, they also have an extended hard tail of emission at high frequencies, which has a power-law spectrum with a spectral index of $\alpha \approx -(p/2) \approx -1.15$. At the bottom of Fig. 6, there is a scale which shows the portion of the electromagnetic spectrum involved.

3.1. EUV and Soft X-ray Emission

Fig. 6 shows that the fluxes from different models all tend to agree at frequencies $\sim 2 \times 10^{16}$ Hz, which corresponds to a photon energy of ~ 80 eV. Thus, EUV and very soft X-ray emission might be expected to be a universal property of clusters of galaxies, if they have all produced populations of relativistic electrons with total energies which are at least $\sim 10^{-2}$ of their thermal energies. The one constraint is that at least a portion of these particles must have been injected at moderate to low redshifts, $z \lesssim 1$. The fact that essentially all of the models produce a strong and similar flux at EUV energies may help to explain the fact the excess EUV emission has been detected in all of the cluster observed with the *Extreme Ultraviolet Explorer (EUVE)* satellite and which lie in directions of sufficiently low Galactic columns that this radiation is observable (Lieu et al. 1996a,b; Mittaz, Lieu, & Lockman 1998; Sarazin & Lieu 1998). Values of $L_\nu(\text{EUV})$ at a frequency of $\nu = 2 \times 10^{16}$ Hz are listed in Table 3 of Sarazin (1999). From these values, one finds that the emission at EUV energies is fairly directly related to $E_{CR,e}^{tot}$, the total amount of energy injected in electrons with $\gamma \geq 300$. The average relationship is about

$$L_\nu(\text{EUV}) \sim 6 \times 10^{27} \left(\frac{E_{CR,e}^{tot}}{10^{63} \text{ ergs}} \right) \text{ ergs.} \quad (4)$$

Models which are likely to apply to real clusters agree with equation (4) to within a factor of 4.

While the amount of EUV emission is fairly constant from model to model, the spectrum depends strongly on the amount of recent particle injection. Very steeply declining spectra occur in models without current particle acceleration and with small values of γ_{max} . For many of the models, the spectral can be fit by a power-law with $-1.5 \gtrsim \alpha_{EUV} \gtrsim -0.6$, but very large negative values also occur. The spectrum drops more rapidly with frequency as the proportion of electrons which are currently being accelerated decreases.

Because the *EUVE* observations of clusters have no spectral resolution, there is no detailed information on the observed spectrum of EUV emission (Lieu et al. 1996a,b; Mittaz, Lieu, & Lockman 1998). However, the ratio of *EUVE* fluxes to those in the softest bands of the *ROSAT* PSPC suggest that the EUV spectra are generally steeply declining. The spectra of the Coma cluster is less steeply declining than that of Abell 1795; this might be understood as the result of particle acceleration by merger shocks, since Coma appears to be undergoing a merger or

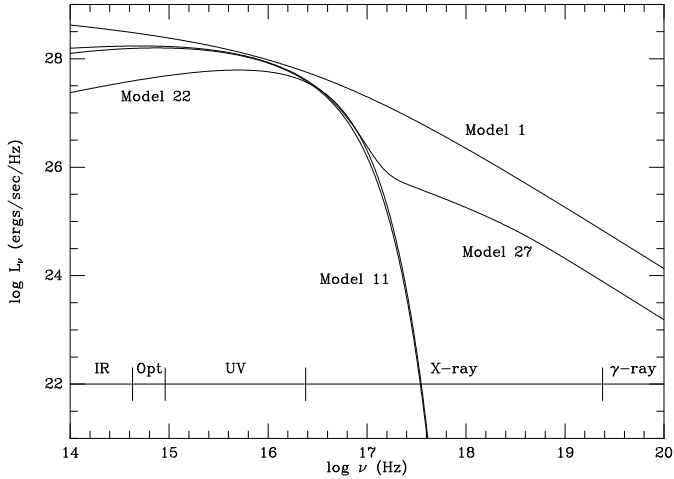


Fig. 6. The IC emission spectra for different types of cluster models (for details on the models, see Sarazin [1999]). Models 1 has current electron acceleration (perhaps due to an ongoing merger shock), but no initial electron population (see Fig. 4). Model 11 has an initial electron population (perhaps due to the formation of the cluster or earlier mergers), but no current electron acceleration (see Fig. 3). Model 22 is identical to Model 11, but the initial electron energy spectrum has a break at an energy of 1 GeV. Model 27 has both an initial electron population, and a source of electrons at present (see Fig. 5). The scale near the bottom of the Figure shows the portion of the electromagnetic spectrum.

mergers (e.g., Burns et al. 1994), while Abell 1795 appears regular and relaxed (e.g., Briel & Henry 1996). Also, the EUV spectra appear to get steeper with increasing radius in the Abell 1795 cluster (Mittaz, Lieu, & Lockman 1998). This might be the result of decreasing gas density with radius, which will decrease the effect of Coulomb loses at low energies (Fig. 2).

3.2. Hard X-ray IC Emission and Radio Halos

At photon energies of 0.5 to 10 keV, the dominant emission in most clusters is the thermal emission from the hot ICM, and IC emission will be difficult to detect. However, at energies $\gtrsim 20$ keV, IC emission should again become observable, assuming that it is dropping as power-law function of frequency, while the thermal emission drops as an exponential. IC emission at photon energies of ~ 50 keV will be produced by electrons with $\gamma \sim 10^4$. These particles have rather short lifetimes ($t_{loss} \ll 10^9$ yr), and are only present in clusters in which there has been substantial electron acceleration since $z \lesssim 0.03$. As Fig. 6 shows, only the models with current or very recent particle acceleration have any significant HXR emission.

Because of the short lifetimes of the particles producing HXR emission, these electrons are likely to be close to steady-state if present in significant quantities. The

expected steady-state spectral index if IC losses dominated would be $\alpha_{HXR} = -(p+1)/2 \approx -1.65$. The best-fit spectral indices are flatter than this, $\alpha_{HXR} \approx -1.1$, mainly because other loss processes are important at the lower energy end of the HXR band (Fig. 1). All of the HXR spectral shapes in the models are very similar, as expected for steady-state populations. The differences in the HXR luminosities just reflect differences in the present rate of electron acceleration. To a good approximation, the present day value of the hard X-ray IC luminosity L_{HXR} (20–100 keV) is simply given by

$$L_{HXR} \approx 0.17 \dot{E}_{CR,e}(\gamma > 5000). \quad (5)$$

where $\dot{E}_{CR,e}(\gamma > 5000)$ is the total present rate of injection of energy in cosmic ray electrons with $\gamma > 5000$. The best-fit coefficient (0.17 in eqn. 5) depends somewhat on the power-law index of the injected electrons; the value of 0.17 applies for $p = 2.3$.

The same relativistic electrons which produce HXR emission by IC scattering will also produce radio emission by synchrotron emission. The synchrotron radio emission from these models is given in Sarazin (1999). Electrons with a Lorentz factor of γ produce radio emission with $\nu \sim 100(B/\mu G)(\gamma/10^4)^2$ MHz, and rather high electron energies ($\gamma \gtrsim 10^4$) are needed to produce observable radio emission. Thus, these are likely to be the same electrons which produce the hardest HXR emission. In general, HXR emission and radio synchrotron emission are expected only in clusters with very recent or current acceleration of relativistic electrons. Thus, both measure the current rate of particle injection. For example, if the particles are accelerated in ICM shocks, HXR and radio emission would be expected only in clusters which are currently undergoing (or which very recently underwent) a merger.

Recently, excess hard X-ray emission has been detected in the Coma (Fusco-Femiano et al. 1999) and Abell 2199 (Kaastra, Bleeker, & Mewe 1998) clusters with *BeppoSAX*. It is tempting to attribute this HXR radiation to IC emission from higher energy electrons. Of course, Coma has a radio halo and abundant evidence for merger activity. Thus, it is consistent with this hypothesis, although the required magnetic field ($B = 0.15 \mu G$) is smaller than might have been expected. On the other hand, Abell 2199 is a relaxed cluster with a strong cooling flow. It has no radio halo emission, with an upper limit on the radio flux which is inconsistent with the IC interpretation of the HXR emission unless $B \lesssim 0.01 \mu G$ (Kempner & Sarazin 1999). Thus, it seems unlikely that the HXR in Abell 2199 is due to IC scattering of CMB photons. It is possible that part of the HXR emission may be due to nonthermal bremsstrahlung (bremsstrahlung from superthermal but not strongly relativistic electrons).

3.3. Optical and UV Emission

One also expects that the lower energy portion of the cosmic ray population in clusters will produce diffuse optical and UV emission. Diffuse optical emission is known to exist in many clusters, particularly in those with central cD galaxies (e.g., Boughn & Uson 1997). Although the origin is not completely understood, the optical colors of the diffuse light suggest that it is due to old stars, which may have been stripped from cluster galaxies. It is likely that the near or vacuum UV are better regions to detect low surface brightness diffuse emission due to IC emission, since the older stellar population in E and S0 galaxies (and, presumably, the intracluster stellar population) are fainter there.

The IC optical-UV emission from the models is given in Sarazin (1999). The predicted fluxes are rather low when compared to the diffuse optical emission seen in clusters of galaxies or to the sensitivity of current and UV instruments for detecting diffuse emission. The UV powers of most of the models lie within a relatively narrow range of about an order of magnitude. Unless the electron density in the ICM is much higher than 0.001 cm^{-3} and Coulomb losses are catastrophic or the electron population in clusters is very old, one would always expect a significant population of lower energy electrons. The IC spectra in the optical and UV are fairly flat, with spectral indices of $-0.5 \gtrsim \alpha_{Opt,UV} \gtrsim 0.3$. In models with current electron acceleration, the lower energy electron population should be approaching steady-state with the Coulomb losses, and the expected power-law for the IC emission is $\alpha \approx -(p-2)/2 \approx -0.15$. For models without current acceleration, the electron spectrum is expected to be nearly flat at low energies, and the $L_\nu \sim \nu^{1/2}$. Thus, the spectral index should be slightly positive in these models.

4. Gamma-Ray Emission

The same relativistic electrons and ions will produce gamma-ray emission. This involves a wide variety of physical processes; in the interest of brevity, only the region around 100 MeV will be discussed here. The two major emission processes in this region of the gamma-ray spectrum are electron bremsstrahlung (due to collisions between relativistic electrons and thermal ions and electrons), and π^0 decay, due to collisions between relativistic ions and thermal ions. Fig. 7 shows the predicted spectrum for the Coma cluster. The electron population was determined by the IC emission required to fit the observed *EUVE* flux and *EUVE/ROSAT* flux ratio (Lieu et al. 1996a). The ratio of the π^0 decay component to the bremsstrahlung component is determined by the ratio of relativistic ions to electrons. In Fig. 7, this ratio was taken to be 10.

The predicted flux of gamma-rays with $h\nu \geq 100$ MeV is about $2 \times 10^{-8} \text{ cts/cm}^2/\text{s}$. For comparison, the

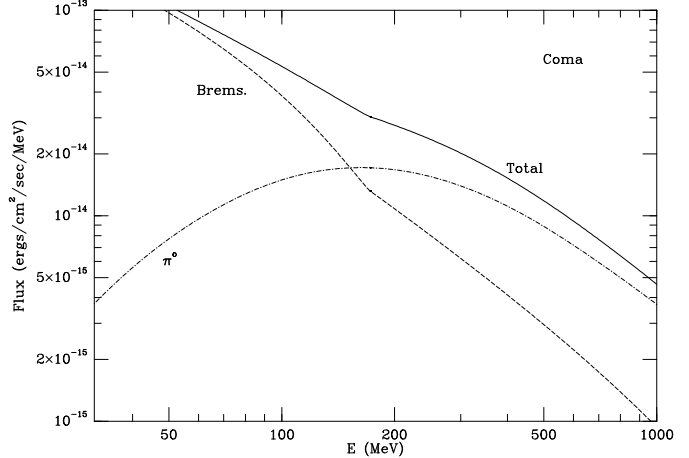


Fig. 7. The predicted gamma-ray spectrum of the Coma cluster in the region around 100 MeV. The emission is mainly the result of bremsstrahlung by relativistic electrons and π^0 decay due to relativistic ions. The electron population was determined by the best-fit *EUVE* fluxes and spectra. The ions have 10 times the electron energy.

EGRET upper limit on the flux from Coma in this range is $\leq 4 \times 10^{-8} \text{ cts/cm}^2/\text{s}$ (Sreekumar et al. 1996). Thus, it seems certain that *GLAST* will detect Coma and many other clusters, assuming that the detected EUV emission from clusters is due to IC from relativistic electrons. The measurement of the gamma-ray spectrum in the region around 100 MeV will allow the ratio of relativistic ions to electrons to be determined. In many astrophysical environments, this is an unknown quantity. The *EGRET* limit already implies that this ratio is $\lesssim 30$ in the Coma cluster.

Acknowledgements. This work was supported in part by NASA Astrophysical Theory Program grant NAG 5-3057. I would like to thank Hans Böhringer and Luigina Feretti for organizing such an enjoyable and useful workshop.

References

- Blandford, R. D., & Eichler, D. 1987, *Phys. Rep.*, 154, 1
- Boughn, S. P., & Uson, J. M. 1997, *ApJ*, 488, 44
- Briel, U. G., & Henry, J. P. 1996, *ApJ*, 472, 131
- Burns, J. O., Roettiger, K., Ledlow, M., & Klypin, A. 1994, *ApJ*, 427, 87
- Colafrancesco, S., & Blasi, P. 1998, *APh*, 9, 227
- Enßlin, T. A., & Biermann, P. L. 1998, *A&A*, 330, 90
- Fusco-Femiano, R., et al., 1999, *ApJ*, 513, L21
- Ginzburg, V. L., & Syrovatskii, S. I. 1964, *The Origin of Cosmic Rays* (New York: MacMillan)
- Giovannini, G., Feretti, L., Venturi, T., Kim, K. T., & Kronberg, P. P. 1993, *ApJ*, 406, 399
- Hwang, C.-Y. 1997, *Science*, 278, 1917
- Kaastra, J. S., Bleeker, J. A. M., & Mewe, R. 1998, *Nucl. Phys. B*, 69, 567
- Kempner, J., & Sarazin, C. L. 1999, *ApJ*, submitted
- Lieu, R., Mittaz, J. P. D., Bowyer, S., Breen, J. O., Murphy, E. M., Lockman, F. J., & Hwang, C.-Y. 1996a, *Science*, 274, 1335

Lieu, R., Mittaz, J. P. D., Bowyer, S., Lockman, F. J., Hwang,

C.-Y., & Schmitt, J. H. M. M. 1996b, *ApJ*, 458, L5

Mittaz, J. P. D., Lieu, R., & Lockman, F. J. 1998, *ApJ*, 498,

L17

Sarazin, C. L. 1999, *ApJ*, 520, in press

Sarazin, C. L., & Lieu, R. 1998, *ApJ*, 494, L177

Sreekumar, P., et al., 1996, *ApJ*, 464, 628